GENERAL PROBLEMS OF THEORETICAL PHYSICS

O.M. KRUPNITSKA

Institute for Condensed Matter Physics, Nat. Acad. of Sci. of Ukraine
(1, Svientsitski Str., Lviv 79011, Ukraine; e-mail: krupnitska@icmp.lviv.ua)

PACS 75.10.Jm

INFLUENCE OF THE HEISENBERG EXCHANGE INTERACTION ANISOTROPY ON THE MAGNETIZATION PROCESS OF A FRUSTRATED DIAMOND CHAIN IN A STRONG MAGNETIC FIELD

A frustrated diamond spin chain in a z- or x-aligned external magnetic field has been considered in the framework of the spin-$\frac{1}{2}$ antiferromagnetic XXZ Heisenberg model. The magnetization process of the frustrated diamond spin chain is analyzed, by using the effective models found in the strong-coupling approximation in the case where the Heisenberg interaction anisotropy parameter $\Delta > 1$. The theory is applied to explain experimental data for natural mineral azurite, $Cu_3(CO_3)_2(OH)_2$.

K e y w o r d s: quantum Heisenberg antiferromagnet, frustrated diamond chain, azurite.

1. Introduction

In recent years, a lot of attention has been paid to the theoretical and experimental studies of the properties of frustrated quantum Heisenberg antiferromagnets [1]. Unlike ferromagnets, the interactions in antiferromagnetic spin systems may compete with one another; this is the so-called frustration. It can be a competition of exchange interactions between two neighbor spins or between a spin and another spin located behind the neighbor one in simple lattices (e.g., the $J_1 - J_2$ model for the square lattice) or between the nearest spins in a lattice with a complicated geometry (e.g., in the kagome lattice).

There exists a wide class of one-, two-, and three-dimensional quantum Heisenberg antiferromagnets, which can be studied in detail, by using special methods. These are the so-called frustrated quantum Heisenberg antiferromagnets with dispersionless (flat) low-energy magnon states. The research of the properties of such spin systems in strong magnetic fields

and at low temperatures is based on the concept of localized magnons [2–6], which allows the problem to be reduced to the consideration of a certain classical lattice gas consisting of hard objects. The characteristic features of spin systems, in which the existence of localized magnons is allowed, are a plateau and a jump in the magnetization curve at the saturation field and $T = 0$ (i.e. in the ground state), the Peierls instability, and the residual entropy at the saturation field. The theory developed in works [2–5] concerns the so-called perfect geometry, when the one-magnon states are strictly localized (the one-magnon band is strictly dispersionless). This theory also predicts the isotropic character of Heisenberg exchange interactions (the anisotropy parameter $\Delta = 1$), when the direction of an applied magnetic field is irrelevant.

In real systems, the conditions that provide a strict localization of magnons can be violated, and Heisenberg exchange interactions can be anisotropic ($\Delta \neq 1$). Then an important question arises: Which are consequences for the observed properties owing to a deviation from the perfect geometry or an arbitrary direction of the applied magnetic field if the Heisen-
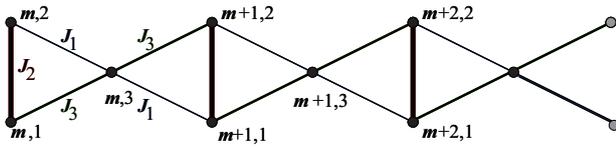
Fig. 1. Frustrated diamond spin chain. The lattice sites are convenient to be enumerated by a pair of indices. The first index enumerates the lattice cells: $m = 1, ..., \mathcal{N}$; where $\mathcal{N} = \frac{N}{3}$, and N is the number of lattice sites. The second index marks the site position in the cell

berg interaction is anisotropic? In other words, how does a theory for such frustrated quantum antiferromagnets look like near the paradigm of localized magnons?

The case of a deviation from the perfect geometry was studied in works [7–9]. In particular, effective Hamiltonians in the strong-coupling approximation were constructed in work [7] to study the properties of a deformed diamond spin chain. This model was improved in work [8]. In work [9], a heuristic ansatz was proposed for the partition function of a deformed diamond spin chain. Those researches analyzed the case of isotropic Heisenberg interaction ($\Delta = 1$).

Within the last decade, a lot of attention has been attracted by the natural mineral azurite, $Cu_3(CO_3)_2(OH)_2$. Its magnetic properties can be described in the framework of the frustrated Heisenberg diamond spin chain model [10–13]. The azurite parameter set corresponds to a model near the perfect geometry, which predicts the existence of localized magnons [14]. In work [11], the results of experimental researches were reported concerning the magnetic properties of azurite at a temperature $T < 4.2$ K and magnetic fields $H = 0 \div 50$ T. In particular, the magnetization curves were measured in a magnetic field applied along the crystallographic axis b and perpendicularly to it. Those curves do not coincide, which can result from the anisotropy of Heisenberg exchange interactions in azurite (see work [12]).

The issue concerning the magnetization of a frustrated diamond chain with the XXZ Heisenberg interaction in an arbitrarily oriented field was formulated in work [15]. However, the analysis was confined to the case where the parameter of exchange interaction anisotropy $0 \leq \Delta < 1$. In particular, the presented results included the magnetization curves for a frustrated Heisenberg anisotropic diamond chain in magnetic fields applied along either the axis x or

the axis z. To describe the system at low temperatures, corresponding effective Hamiltonians were constructed in the strong-coupling approximation. The obtained models turned out exactly solvable, namely, spin-$\frac{1}{2}$ XY chains in an external transverse field. For such spin chains, the Jordan–Wigner fermionization method is applicable [16].

In this work, a frustrated XXZ Heisenberg diamond chain in a magnetic field oriented along one of the axes x and z will be considered in the case $\Delta > 1$ for the parameter of Heisenberg exchange interaction anisotropy. Effective models for this spin chain will also be constructed in the strong-coupling approximation. The magnetization curves at low temperatures will be obtained, and their characteristic features will be analyzed as functions of the anisotropy parameter Δ. The developed theory will be applied to determine the parameter Δ for azurite on the basis of experimental data presented in works [10–12].

2. Effective Theory

Let us apply the spin-$\frac{1}{2}$ antiferromagnetic model with the anisotropic Heisenberg interaction to a frustrated diamond chain (Fig. 1). The corresponding Hamiltonian looks like

$$H = \sum_{(ij)} J_{ij} \left(s_i^x s_j^x + s_i^y s_j^y + \Delta s_i^z s_j^z \right) - h \sum_{i=1}^{N} s_i^\alpha, \quad (1)$$
$$\alpha = x, z,$$

where the summation in the first term is carried out over only the neighbor lattice sites, whereas that in the second one is extended over all N lattice sites (see Fig. 1). In addition, $J_{ij} > 0$ and $\Delta \geq 1$. If $J_2 > 0$ is the largest antiferromagnetic exchange interaction, only two states of the vertical J_2-bond are expected to play a certain role in low-temperature properties under strong magnetic fields. This circumstance allows the initial frustrated quantum spin system to be effectively described within a simpler two-state model. In practice, such efficient theories can be developed using the strong-coupling approximation [7, 17].

Two cases will be considered: if the external magnetic field is directed (i) along the axis z or (ii) along the axis x. In the former case, Hamiltonian (1) with $\alpha = z$ is used. If the magnetic field is applied along the axis x, a unitary transformation of the initial Hamiltonian (1) should be made to obtain a Hamiltonian with anisotropic interaction in a magnetic field

directed along the axis z,

$$H = \sum_{(ij)} J_{ij} \left[\mathbf{s}_i \cdot \mathbf{s}_j + (\Delta - 1) s_i^x s_j^x \right] - h \sum_i s_i^z. \quad (2)$$

The strong-coupling approximation is based on the assumption that the interaction J_2 dominates, i.e. $J_i/J_2 \ll 1$, where $i \neq 2$. Therefore, the Hamiltonian H can be divided into a "major" part H_{main} and a "perturbation" V: $H = H_{\mathrm{main}} + V$. Here, H_{main} is the Hamiltonian describing the interaction between two spins at the vertical bond with the constant J_2 and the Zeeman interaction of all spins with the magnetic field h_0 (see below). In strong magnetic fields, only two of four states at the vertical bond are taken into consideration; these are the states $|u\rangle$ and $|d\rangle$ with the energies ε_u and ε_d, respectively. Note that $\varepsilon_u = \varepsilon_d$ at $h = h_0$. The ground state $|\varphi_0\rangle$ of Hamiltonian H_{main} is $2^{\mathcal{N}}$-fold degenerate; here, $\mathcal{N} = N/3$ is the number of chain cells. Let us introduce the operator P of projection on the model space formed by the $2^{\mathcal{N}}$-fold degenerate ground state:

$$P = |\varphi_0\rangle\langle\varphi_0| = \otimes_{m=1}^{\mathcal{N}} \left[(|u\rangle\langle u| + |d\rangle\langle d|) \otimes | \uparrow_3 \rangle\langle \uparrow_3 | \right]_m. \quad (3)$$

For $J_i \neq 0$, $i \neq 2$, and $h - h_0 \neq 0$, we construct an effective Hamiltonian that operates only in the model space, but gives the exact energy of the ground state for the Hamiltonian H. By applying the perturbation theory, we obtain [18]

$$H_{\mathrm{eff}} = PHP + PV \sum_{\alpha \neq 0} \frac{|\varphi_\alpha\rangle\langle\varphi_\alpha|}{\varepsilon_0 - \varepsilon_\alpha} VP + \dots . \quad (4)$$

First, let us consider the case where the magnetic field is applied along the axis z. In strong magnetic fields, we consider the following two states at the vertical bond: the completely polarized state $|u\rangle = | \uparrow_1 \uparrow_2 \rangle$ with the energy $\varepsilon_u = \Delta \frac{J_2}{4} - h$ and the one-magnon state $|d\rangle = \frac{1}{\sqrt{2}}(| \uparrow_1 \downarrow_2 \rangle - | \downarrow_1 \uparrow_2 \rangle)$ with the energy $\varepsilon_d = -\frac{J_2}{2} - \frac{\Delta J_2}{4}$. The effective Hamiltonian is convenient to be written in terms of the (pseudo)-spin-$\frac{1}{2}$ operators T, which are defined as follows: $T^z = \frac{1}{2}(|u\rangle\langle u| - |d\rangle\langle d|)$, $T^+ = |u\rangle\langle d|$, and $T^- = |d\rangle\langle u|$. In terms of the (pseudo)spin-$\frac{1}{2}$ operators, the first term on the right-hand side of Eq. (4) looks like

$$PHP = \sum_{m=1}^{\mathcal{N}} \left[-\frac{J_2}{4} - h + \Delta \frac{J}{2} - (h - h_1) T_m^z \right], \quad (5)$$

where $h_1 = h_0 + \Delta J$, $h_0 = J_2 \sqrt{\frac{1+\Delta}{2}}$, and $J = \frac{J_1 + J_3}{2}$. To find the second term on the right-hand side of formula (4), we should consider $\mathcal{N} \times 2^{\mathcal{N}}$ excited states $|\varphi_\alpha\rangle$ – these are states with one flipped spin at the site connecting two neighbor cells (see Fig. 1) – with the energy $\varepsilon_\alpha = \varepsilon_0 + h_0$. Then we have

$$PV \sum_{\alpha \neq 0} \frac{|\varphi_\alpha\rangle\langle\varphi_\alpha|}{\varepsilon_0 - \varepsilon_\alpha} VP = -\frac{(J_1 - J_3)^2}{4J_2(\Delta + 1)} \times$$
$$\times \sum_m \left[1 - 2T_m^z - 2 \left(T_m^x T_{m+1}^x + T_m^y T_{m+1}^y \right) \right]. \quad (6)$$

Therefore, we obtain the following expression for the effective Hamiltonian H_{eff} [Eq. (4)] in the strong-coupling approximation:

$$H_{\mathrm{eff}} = \sum_m \left[\mathsf{C} - \mathsf{h} T_m^z + \mathsf{J} \left(T_m^x T_{m+1}^x + T_m^y T_{m+1}^y \right) \right], \quad (7)$$

where

$$\mathsf{C} = -h - \frac{J_2}{4} + \Delta \frac{J}{2} - \frac{(J_3 - J_1)^2}{4(1+\Delta)J_2}, \quad J = \frac{J_3 + J_1}{2},$$

$$\mathsf{h} = h - h_1 - \frac{(J_3 - J_1)^2}{2(1+\Delta)J_2}, \quad h_1 = \frac{1+\Delta}{2} J_2 + \Delta J,$$

$$\mathsf{J} = \frac{(J_3 - J_1)^2}{2(1+\Delta)J_2}.$$

In the limit of isotropic Heisenberg interaction, $\Delta = 1$, the obtained effective Hamiltonian (7) coincides with the results of works [7, 8]. In addition, in the limit where $\Delta \to \infty$ but $J_i \Delta = I_i < \infty$, we obtain $\mathsf{C} \to -h + \frac{1}{4}(I_1 + I_3)$, $\mathsf{h} \to h - \frac{1}{2}(I_1 + I_2 + I_3)$, and $\mathsf{J} \propto \frac{1}{\Delta^2} \to 0$. Hence, in this limit, the effective model (7) is reduced to the model of free spins in an external magnetic field.

Now, let us consider the case where the magnetic field is applied along the axis x. Hamiltonian (2) is used. In a strong magnetic field, we consider the following two states at every vertical bond:

$$|u\rangle = \alpha | \uparrow_1 \uparrow_2 \rangle + \beta | \downarrow_1 \downarrow_2 \rangle, \quad (8)$$

Here,

$$\alpha = \frac{1}{C} \frac{\Delta - 1}{4} J_2,$$

$$\beta = \frac{1}{C} \left[h - \sqrt{\frac{(\Delta - 1)^2}{16} J_2^2 + h^2} \right],$$

$$C = \sqrt{2} \sqrt{\frac{(\Delta - 1)^2}{16} J_2^2 - h \sqrt{\frac{(\Delta - 1)^2}{16} J_2^2 + h^2} + h^2}.$$

with the energy $\varepsilon_u = \frac{1}{4}[J_2 - \sqrt{(\Delta - 1)^2 J_2^2 + 16h^2}]$ and

$$|d\rangle = \frac{1}{\sqrt{2}}\left(|\uparrow_1\downarrow_2\rangle - |\downarrow_1\uparrow_2\rangle\right) \qquad (9)$$

with the energy $\varepsilon_d = -\frac{1}{4}(2+\Delta)J_2$. For the first term on the right-hand side of formula (4), we obtain

$$PHP = \sum_m \left[-\frac{h}{2} - \frac{2+\Delta}{4}J_2 - \right.$$
$$\left. - (h - h_0 - J)(\alpha^2 - \beta^2)\left(\frac{1}{2} + T_m^z\right) \right], \qquad (10)$$

where $J = \frac{J_1 + J_3}{2}$, $h_0 = J_2\sqrt{\frac{1+\Delta}{2}}$, and the constants α and β were defined in formulas (8). There are two classes of excited states that make a contribution to the second term on the right-hand side of Eq. (4). One of them includes $\mathcal{N} \times 2^{\mathcal{N}}$ states with one flipped spin at the third site that connects two neighbor cells (see Fig. 1). Therefore,

$$PV\sum_{\alpha_1 \neq 0} \frac{|\varphi_{\alpha_1}\rangle\langle\varphi_{\alpha_1}|}{\varepsilon_0 - \varepsilon_{\alpha_1}} VP =$$
$$= \sum_m \left(\mathsf{C}_1 - \mathsf{h}_1 T_m^z + \mathsf{J}^x T_m^x T_{m+1}^x + \mathsf{J}^y T_m^y T_{m+1}^y \right), \quad (11)$$

where

$$\mathsf{C}_1 = -\frac{(J_3 - J_1)^2}{16h_0}\left[1 + 2\alpha\beta(1 - \Delta^2) + \Delta^2\right],$$

$$\mathsf{h}_1 = -\frac{(J_3 - J_1)^2}{4h_0}(\alpha^2 - \beta^2)\Delta,$$

$$\mathsf{J}^x = \frac{(J_3 - J_1)^2}{4h_0}(\alpha - \beta)^2\Delta^2,$$

$$\mathsf{J}^y = \frac{(J_3 - J_1)^2}{4h_0}(\alpha + \beta)^2.$$

The other class of excited states includes $\mathcal{N} \times 2^{\mathcal{N}-1}$ states. In this case, the dimer state of the m-th cell equals $-\beta|\uparrow_1\uparrow_2\rangle + \alpha|\downarrow_1\downarrow_2\rangle$, and its energy $\frac{1}{4}[J_2 + \sqrt{(\Delta - 1)^2 J_2^2 + 16h^2}]$, where the constants α and β are indicated in formulas (8). The energy of those excited states is $\varepsilon_{\alpha_2} = \varepsilon_0 + \frac{1}{2}(3 + \Delta)J_2$. It is easy to verify that

$$PV\sum_{\alpha_2 \neq 0} \frac{|\varphi_{\alpha_2}\rangle\langle\varphi_{\alpha_2}|}{\varepsilon_0 - \varepsilon_{\alpha_2}} VP =$$
$$= -\sum_m \frac{8(h - h_0 - J)^2}{(3 + \Delta)J_2}\alpha^2\beta^2\left(\frac{1}{2} + T_m^z\right). \qquad (12)$$

Combining formulas (10), (11), and (12), we obtain H_{eff}. The effective Hamiltonian for the frustrated XXZ Heisenberg diamond spin chain in a magnetic field directed along the axis x and at $\Delta \geq 1$ looks like

$$H_{\text{eff}} = \sum_m \left(\mathsf{C} - \mathsf{h}T_m^z + \mathsf{J}^x T_m^x T_{m+1}^x + \mathsf{J}^y T_m^y T_{m+1}^y \right), \quad (13)$$

where

$$\mathsf{C} = -\frac{h}{2} - \frac{2+\Delta}{4}J_2 - \frac{1}{2}(h - h_0 - J)(\alpha^2 - \beta^2) -$$
$$- \frac{(J_3 - J_1)^2}{16h_0}\left[1 + 2\alpha\beta(1 - \Delta^2) + \Delta^2\right] -$$
$$- \frac{4(h - h_0 - J)^2}{(3 + \Delta)J_2}\alpha^2\beta^2,$$

$$\mathsf{h} = (h - h_0 - J)(\alpha^2 - \beta^2) -$$
$$- \frac{(J_3 - J_1)^2}{4h_0}(\alpha^2 - \beta^2)\Delta + \frac{8(h - h_0 - J)^2}{(3 + \Delta)J_2}\alpha^2\beta^2,$$

$$\mathsf{J}^x = \frac{(J_3 - J_1)^2}{4h_0}(\alpha - \beta)^2\Delta^2,$$

$$\mathsf{J}^y = \frac{(J_3 - J_1)^2}{4h_0}(\alpha + \beta)^2.$$

In the limit $\Delta \to 1$, the effective Hamiltonians (7) and (13) coincide and correspond to an unfrustrated spin-$\frac{1}{2}$ isotropic XY chain in a transverse magnetic field. For a perfect frustrated diamond chains ($J_1 = J_3$), in the limit $\Delta \to \infty$ but $J_i\Delta = I_i < \infty$, the effective Hamiltonian (13) is reduced to the model of free spins in an external magnetic field: $\mathsf{J}^x = 0$ and $\mathsf{J}^y = 0$.

Formally, the expressions for the effective Hamiltonians (7) and (13) are identical to those obtained earlier in work [15] in the case $0 \leq \Delta < 1$. However, they describe a qualitatively different case where the parameter of Heisenberg exchange interaction anisotropy $\Delta > 1$. In the latter case, the expressions for the constants α and β differ from those in work [15] [cf. expressions (8) for the constants α and β with the corresponding expressions in work [15]]. The obtained models (7) and (13) can be exactly solved, by using the Jordan–Wigner fermionization method [16].

3. Comparison of Initial and Effective Models

To study the obtained effective models (7) and (13), we compare their predictions with the data for initial models. As an example, let us consider the low-temperature magnetization curves for a frustrated diamond spin chain in a magnetic field applied along either the axis x or the axis z (see Figs. 2 and
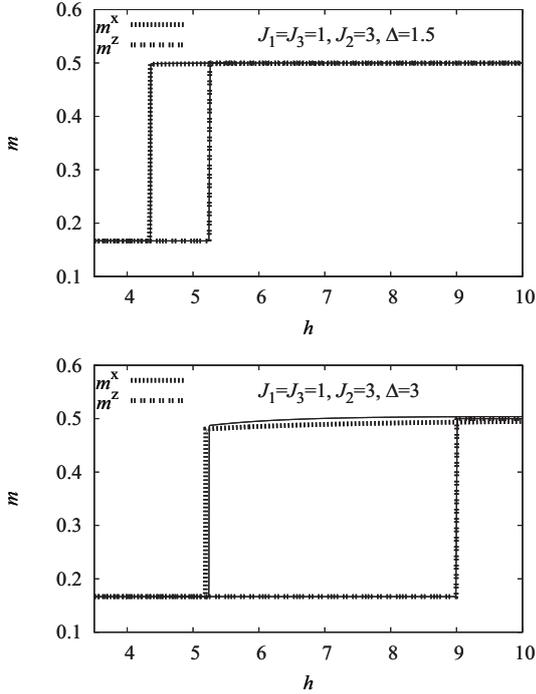
Fig. 2. Magnetization curves for the frustrated Heisenberg diamond spin chain with the parameters $J_1 = J_3 = 1$, $J_2 = 3$, $\Delta = 1.5$ (the upper panel) and 3 (the lower panel) in the magnetic field directed along the axis z or x (the dotted curves). The exact diagonalization data were obtained for a finite periodic chain with $N = 15$. Thin black curves illustrate the results obtained for infinitely large systems on the basis of effective theory and with the use of the Jordan–Wigner fermionization

Fig. 3. The same that in Fig. 2, but for $J_1 = 0.85$, $J_2 = 3$, and $J_3 = 1.15$

3). The results can be obtained, by using the exact-diagonalization method [19]. For this purpose, a chain with $N = 15$ sites and periodic boundary conditions will be considered. The parameters are $J_2 = 3$, $\Delta = 1.5$ and 3, and the low temperature $T = 0.001$. The other parameters are $J_1 = J_3 = 1$ for the perfect geometry, and $J_1 = 0.85$ and $J_3 = 1.15$ for the nonperfect one.

If the parameter of Heisenberg interaction anisotropy $\Delta = 1$, the magnetization curves for a diamond chain in a magnetic field applied along either the axis x or the axis z evidently coincide. However, if Δ differs from 1, e.g., if $\Delta = 1.5$ or 3, the magnetization curves are different for different magnetic orientations. In the perfect geometry case (see Fig. 2), the magnetization curve has a vertical jump at a characteristic magnetic field h_*. If the magnetic field is applied along the axis z, h_* is a field, at which the mag-
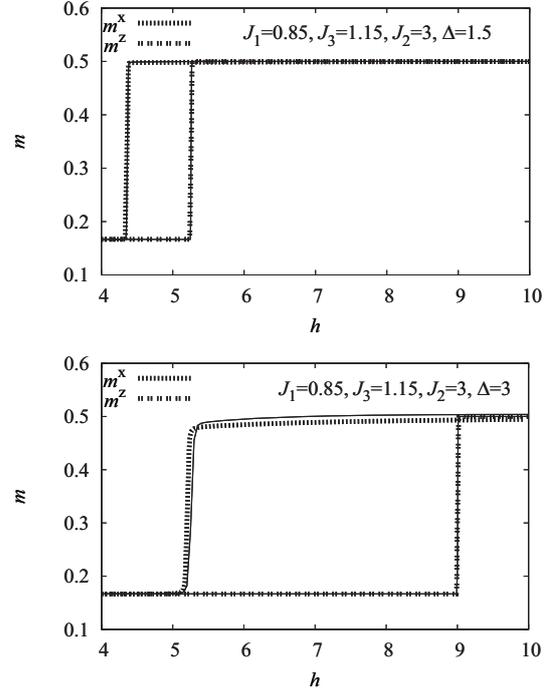
netization saturates, i.e. $m(h_* + 0) = \frac{1}{2}$. If the magnetic field is applied along the axis x, the magnetization saturation is achieved only in the limit $h \to \infty$; however, at $h = h_* + 0$, the chain magnetization is close to $\frac{1}{2}$. An expression for the characteristic field h_* can be derived from the condition $\mathsf{h}(h_*) = 0$ [15]. If the magnetic field is applied along the axis z,

$$h_*^z = \frac{1 + \Delta}{2} J_2 + \Delta J + \frac{(J_3 - J_1)^2}{2(1 + \Delta)J_2}. \tag{14}$$

Accordingly, for the field applied along the axis x, we have

$$h_*^x \approx \sqrt{\frac{1 + \Delta}{2}} J_2 + J + \frac{(J_3 - J_1)^2}{4\sqrt{\frac{1+\Delta}{2}} J_2} \Delta. \tag{15}$$

Those formulas, which were obtained in work [15] when considering the case $0 \leq \Delta < 1$, remain also valid at $\Delta > 1$.

Figure 4 demonstrates the dependence of the magnitude $\Delta m^x = m^x(h_*^x + 0) - m^x(h_*^x - 0)$ of the jump observed in the magnetization curve on the parameter Δ, when magnetic field is applied along the axis
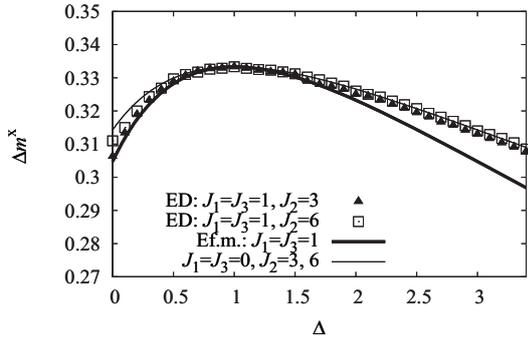
Fig. 4. Magnetization jump $\Delta m^x = m^x(h^x_* + 0) - m^x(h^x_* - 0)$ for the frustrated XXZ Heisenberg diamond chains as a function of the parameter Δ in the magnetic field directed along the axis x for various parameters
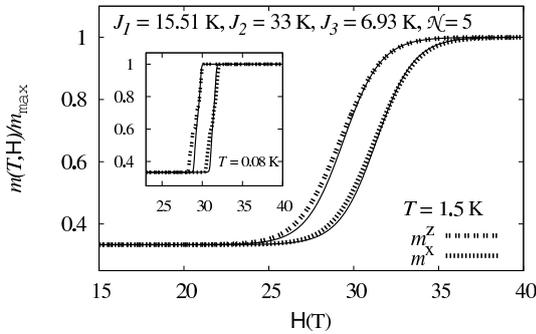

Fig. 5. Low-temperature magnetization curves for the frustrated diamond chains with the azurite parameters $J_1 = 15.51$ K, $J_2 = 33$ K, $J_3 = 6.93$ K ($J_m = 0$), and the gyromagnetic ratio $g = 2.06$ in the magnetic field applied along the axis z or x (dotted curves). Thin black curves illustrate the results obtained on the basis of effective theory and with the use of the Jordan–Wigner fermionization

x. The relevant parameters are $J_2 = 3$ and $J_1 = J_3 = 1$ or 0. Let us consider the case $J_1 = J_3 = 0$, so that $h^x_* = h_0$. Then a simple formula can be obtained for the magnetization of a set of vertical dimers with the interaction J_2 and free spins at the sites $m, 3$. Really, in a strong magnetic field for the magnetic moment of a cell consisting of three sites, we have

$$(\alpha\langle\uparrow\uparrow| + \beta\langle\downarrow\downarrow|)(s^z_1 + s^z_2)(\alpha|\uparrow\uparrow\rangle + \beta|\downarrow\downarrow\rangle) + \frac{1}{2} =$$
$$= (\alpha\langle\uparrow\uparrow| + \beta\langle\downarrow\downarrow|)(\alpha|\uparrow\uparrow\rangle - \beta|\downarrow\downarrow\rangle) + \frac{1}{2} =$$
$$= \alpha^2 - \beta^2 + \frac{1}{2}. \tag{16}$$

Therefore, for the magnetization per site, we obtain $m^x(h_0 + 0) = \frac{\alpha^2-\beta^2}{3} + \frac{1}{6}$. Since $m^x(h_0 - 0) = \frac{1}{6}$, the

jump $\Delta m^x \equiv m^x(h_0 + 0) - m^x(h_0 - 0) = \frac{\alpha^2-\beta^2}{3} \neq 0$ takes place for any Δ (a thin curve in Fig. 4). In the case with interactions, $J_1 = J_3 \neq 0$, and perfect geometry, the magnetization curves can be numerically calculated, by using the exact diagonalization for the diamond chain with the parameters $J_2 = 3$ and $J_1 = J_3 = 1$ (triangles and squares in Fig. 4). In addition, Δm^x can be found, by using the effective model (13) (a bold curve in Fig. 4). The effective model at $J_1 = J_3$ corresponds to the model of free spins in an external magnetic field.

From Fig. 4, one can see that, as Δ increases from 0 to ∞, the jump in the magnetization curve increases to a maximum of $\frac{1}{3}$ at $\Delta = 1$ and then decreases, by tending to zero.

In the case of non-perfect geometry ($J_1 \neq J_3$) and the magnetic field directed along either the axis x or the axis z, the jump in the magnetization curve is smeared, and the magnetization drastically changes in a vicinity of h_* (see Fig. 3). However, the characteristic fields h^z_* and h^x_* remain well determined in this case as well.

4. Application to Azurite

The model of deformed diamond spin chain [see formula (1) and Fig. 1] with the parameters $J_1 \approx 15.51$ K, $J_2 \approx 33$ K, and $J_3 \approx 6.93$ K [14] (in addition, $h = g\mu_B H$, where $g \approx 2.06$, $\mu_B \approx 0.67171$ K/T, and the magnetic field H is reckoned in the Tesla units) is considered to be the most suitable for azurite. Work [12] contains the experimental curve for the azurite magnetization at the temperature $T = 1.5$ K in a magnetic field applied both along the crystallographic b-axis and perpendicularly to it. In the former case, the magnetization curve has a plateau equal to $\frac{1}{3}$ times the magnetization saturation value and located between $H^\parallel_{c1} = 16$ T and $H^\parallel_{c2} = 26$ T; then it drastically increases and saturates at $H^\parallel_{c3} = 32.5$ T. In the case where the field is applied normally to the axis b, the magnetization curve has a plateau equal to $\frac{1}{3}$ times the magnetization saturation value and located between $H^\perp_{c1} = 11$ T and $H^\perp_{c2} = 30$ T; then it drastically increases and saturates at $H^\perp_{c3} = 32.5$ T.

With the help of formulas (14) and (15), it is possible to evaluate the parameter of exchange interaction anisotropy Δ for azurite on the basis of experimental data [11]. Let the condition H $\parallel$ b cor-

respond to the magnetic field H directed along the axis z. Then, using the experimental value of the magnetic field, at which the magnetization curve has a jump, $H^{\parallel} \approx 29$ T, the azurite parameters, and formula (14), we obtain $\Delta \approx 0.85$ for azurite. On the other hand, the condition $H \perp b$ corresponds to the case where the magnetic field is directed along the axis x. The field, at which the magnetization curve has a jump, equals $H^{\perp} \approx 31$ T. Then, from formula (15), we obtain $\Delta \approx 0.84$ for the parameter of exchange interaction anisotropy in azurite. Hence, the theory predicts $\Delta \approx 0.84 \div 0.85$ for the parameter of exchange interaction anisotropy in azurite.

The magnetization curves calculated for the azurite parameters and two temperatures $T = 0.08$ and 1.5 K are depicted in Fig. 5. Note that, for the agreement with experimental data to be better, the interaction J_m between the sites $m, 3$ and $m + 1, 3$ (see Fig. 1) and the interaction between the chains [6] should be taken into consideration. However, these researches go beyond the scope of this work.

5. Conclusions

The influence of the Heisenberg exchange interaction anisotropy on low-temperature properties of an almost flat-band diamond spin chain in a strong magnetic field directed along either the axis x or the axis z has been studied. The analysis is done in the case where the parameter of Heisenberg anisotropy $\Delta > 1$, and it supplements the research carried out earlier for the case $0 \leq \Delta < 1$ [15].

To describe the low-temperature properties of deformed diamond chains in an arbitrarily oriented magnetic field, effective Hamiltonians are constructed in the strong-coupling approximation. The obtained low-temperature magnetization curves agree well at strong fields with the results of exact diagonalization for the initial diamond chain consisting of 15 sites.

The dependence of the magnetization jump magnitude Δm^x on the parameter of Heisenberg exchange interaction anisotropy Δ is obtained for a diamond spin chain in a magnetic field directed along the axis x. The magnetization jump Δm^x is found to be maximum in the isotropic case $\Delta = 1$. On the other hand, $\Delta m^x \to 0$ at $\Delta \to \infty$.

The proposed effective models allow theoretical predictions to be made concerning the low-temperature properties of azurite in strong magnetic fields

(higher than 30 T). The parameter of Heisenberg exchange interaction anisotropy for azurite is evaluated to equal $\Delta \approx 0.84 \div 0.85$.

The developed approach can also be applied to explain experimental data for other frustrated quantum antiferromagnets with almost dispersionless low-energy magnon states, e.g., for the recently synthesized magnetic compound $Ba_2CoSi_2O_6Cl_2$ [20].

1. G. Misguich and C. Lhuillier, in *Frustrated Spin Systems*, edited by H.T. Diep (World Scientific, Singapore, 2005), p. 229; J. Richter, J. Schulenburg, and A. Honecker, in *Quantum Magnetism, Lecture Notes in Physics,* edited by U. Schollwöck, J. Richter, D.J.J. Farnell, and R.F. Bishop (Springer, Berlin, 2004), Vol. 645, p. 85.

2. J. Schulenburg, A. Honecker, J. Schnack, J. Richter, and H.-J. Schmidt, Phys. Rev. Lett. **88**, 167207 (2002).

3. M.E. Zhitomirsky and H. Tsunetsugu, Phys. Rev. B **70**, 100403(R) (2004).

4. O. Derzhko and J. Richter, Eur. Phys. J. B **52**, 23 (2006).

5. O. Derzhko, J. Richter, A. Honecker, and H.-J. Schmidt, Fiz. Nizk. Temp. **33**, 982 (2007).

6. O. Derzhko, J. Richter, and M. Maksymenko, Int. J. Mod. Phys. B **29**, 1530007 (2015).

7. A. Honecker, S. Hu, R. Peters, and J. Richter, J. Phys.: Condens. Matter **23**, 164211 (2011).

8. O. Derzhko, J. Richter, O. Krupnitska, and T. Krokhmalskii, Phys. Rev. B **88**, 094426 (2013); Fiz. Nizk. Temp. **40**, 662 (2014).

9. O. Derzhko, J. Richter, and O. Krupnitska, Cond. Matter Phys. **15**, 43702 (2012).

10. H. Kikuchi, Y. Fujii, M. Chiba, S. Mitsudo, T. Idehara, T. Tonegawa, K. Okamoto, T. Sakai, T. Kuwai, and H. Ohta, Phys. Rev. Lett. **94**, 227201 (2005).

11. H. Kikuchi, Y. Fujii, M. Chiba, S. Mitsudo, T. Idehara, T. Tonegawa, K. Okamoto, T. Sakai, T. Kuwai, K. Kindo, A. Matsuo, W. Higemoto, K. Nishiyama, M. Horvatić, and C. Bertheir, Prog. Theor. Phys. Suppl. **159**, 1 (2005).

12. H. Kikuchi, Y. Fujii, M. Chiba, S. Mitsudo, T. Idehara, T. Tonegawa, K. Okamoto, T. Sakai, T. Kuwai, and H. Ohta, Phys. Rev. Lett. **97**, 089702 (2006).

13. N. Ananikian, H. Lazaryan, and M. Nalbandyan, Eur. Phys. J. B **85**, 223 (2012).

14. H. Jeschke, I. Opahle, H. Kandpal, R. Valenti, H. Das, T. Saha-Dasgupta, O. Janson, H. Rosner, A. Brühl, B. Wolf, M. Lang, J. Richter, S. Hu, X. Wang, R. Pe-

ters, T. Pruschke, and A. Honecker, Phys. Rev. Lett. **106**, 217201 (2011).

15. J. Richter, O. Krupnitska, T. Krokhmalskii, and O. Derzhko, J. Magn. Magn. Mater. **379**, 39 (2015).

16. E. Lieb, T. Schultz, and D. Mattis, Ann. Phys. (N.Y.) **16**, 407 (1961).

17. A. Honecker and A. Läuchli, Phys. Rev. B **63**, 174407 (2001).

18. P. Fulde, *Electron Correlations in Molecules and Solids* (Springer-Verlag, Berlin, 1993).

19. A. F. Albuquerque *et al.*, J. Magn. Magn. Mater. **310**, 1187 (2007); B. Bauer *et al.*, J. Stat. Mech. P05001 (2011).

20. H. Tanaka, N. Kurita, M. Okada, E. Kunihiro, Y. Shirata, K. Fujii, H. Uekusa, A. Matsuo, K. Kindo, and H. Nojiri, J. Phys. Soc. Jpn. **83**, 103701 (2014).

O.M. Крупніцька

ВПЛИВ АНІЗОТРОПІЇ
ОБМІННОЇ ВЗАЄМОДІЇ ГАЙЗЕНБЕРГА
НА ПРОЦЕС НАМАГНІЧЕННЯ ФРУСТРОВАНОГО
РОМБІЧНОГО ЛАНЦЮЖКА У СИЛЬНОМУ
МАГНІТНОМУ ПОЛІ

Р е з ю м е

Розглядається спін-$\frac{1}{2}$ антиферомагнітна XXZ модель Гейзенберга на фрустрованому ромбічному ланцюжку в зовнішньому магнітному полі, прикладеному вздовж осі x або вздовж осі z. Використовуючи ефективні моделі, знайдені в наближенні сильного зв'язку для випадку взаємодії Гейзенберга з параметром анізотропії $\Delta > 1$, досліджено процес намагнічення фрустрованого ромбічного спінового ланцюжка. Теорія застосована до пояснення експериментальних даних для природного мінералу азуриту $Cu_3(CO_3)_2(OH)_2$.